# Formation and Characterization of the ($\eta^2$-$N_2$)Sc(H)OH and ($\eta^1$-NN)$_x$Sc(H)OH ($x = 1, 2$) Complexes in Solid Argon

**Mohua Chen, Guanjun Wang, Gongyu Jiang, and Mingfei Zhou***

*Department of Chemistry & Laser Chemistry Institute, Shanghai Key Laboratory of Molecular Catalysts and Innovative Materials, Fudan University, Shanghai 200433, People's Republic of China*

*Received: October 7, 2004; In Final Form: November 10, 2004*

Hydrido scandium hydroxide dinitrogen complexes, ($\eta^2$-$N_2$)Sc(H)OH and ($\eta^1$-NN)$_x$Sc(H)OH ($x = 1, 2$), have been prepared by the reactions of laser-ablated scandium atoms with $H_2O/N_2$ mixtures in solid argon. The end-on bonded ($\eta^1$-NN)$_x$Sc(H)OH ($x = 1, 2$) complexes were formed spontaneously on annealing, whereas the side-bonded ($\eta^2$-$N_2$)Sc(H)OH complex was generated on broad-band irradiation. These complexes were characterized by infrared absorption spectroscopy as well as density functional theoretical calculations.

## Introduction

Chemical transformation of dinitrogen to ammonia is one of the most important and challenging processes in chemistry.[1] To search for and design efficient catalysts for the reaction of molecular nitrogen and hydrogen yielding ammonia is a very active field of research. The N−N triple bond in a bare $N_2$ molecule has a very high bond energy, which makes the activation very difficult. Dinitrogen binding to the transition metal center elongates the N−N bond and makes it potentially active. Many studies have indicated that a coordinated dinitrogen is reactive to a variety of reagents to generate a N−H bond, and hundreds of different transition metal−dinitrogen complexes have been characterized.[2−5]

The processes of catalytic synthesis of ammonia from nitrogen and hydrogen molecules consist of a complicated sequence of elementary reactions. The reaction mechanisms of nitrogen hydrogenation with and without the presence of transition metal oxides have been investigated theoretically.[6−9] Recent studies by Hwang and Mebel have demonstrated that scandium monoxide (ScO) enhanced the reaction of nitrogen hydrogenation; the $\eta^1$- and $\eta^2$-coordinated complexes, ($\eta^2$-$N_2$)Sc(H)OH and ($\eta^1$-NN)Sc(H)OH, are important intermediates in the ScO ($^2\Sigma^+$) + $N_2$ + $H_2$ → $N_2H_2ScO$ reaction.[9] These complexes should be detected in matrix isolation experiments involving $ScO/N_2/H_2$.

Matrix isolation infrared spectroscopy has proved to be an effective method for characterization of transition metal complexes with weakly bound ligands. Recent investigations on the reactions of transition metal atoms and compounds with dinitrogen molecules have characterized a series of transition metal dinitrogen complexes in solid matrixes.[10−15] In this paper, we report a combined matrix-isolation infrared absorption spectroscopic and density functional theoretical study of the hydridoscandium hydroxide dinitrogen complexes: ($\eta^2$-$N_2$)Sc(H)OH and ($\eta^1$-NN)$_x$Sc(H)OH ($x = 1, 2$). These complexes were generated by the reactions of laser-ablated scandium atoms with $H_2O/N_2$ mixtures in solid argon.

## Experimental and Computational Methods

The experimental setup for pulsed laser ablation and matrix isolation infrared spectroscopic investigation has been described previously.[16] Briefly, the 1064 nm Nd:YAG laser fundamental (Spectra Physics, DCR 150, 20 Hz repetition rate and 8 ns pulse width) was focused onto the rotating scandium metal target through a hole in a CsI window, which was mounted on a cold tip of a closed-cycle helium refrigerator (Air Products, Model CSW202). Typically, 5−10 mJ/pulse laser energy was used. The ablated metal atoms were co-deposited with the $H_2O/N_2$ mixtures in excess argon onto the 12 K CsI window for 1−2 h at a rate of approximately 5 mmol/h. $H_2O$ was subjected to several freeze−pump−thaw cycles to minimize possible atmospheric contamination. The isotopic substituted $^{15}N_2$, $D_2O$, and $H_2{}^{18}O$ and selected mixtures were used in different experiments. Infrared spectra were recorded on a Bruker IFS113v spectrometer at 0.5 cm$^{-1}$ resolution with a DTGS detector in the spectral range of 400−4000 cm$^{-1}$. Matrix samples were annealed at different temperatures, and selected samples were subjected to broad-band irradiation using a 250 W high-pressure mercury arc lamp.

Density functional calculations were performed using the Gaussian 03 program.[17] The most popular Becke's three-parameter hybrid functional, with additional correlation corrections due to Lee, Yang, and Parr, was utilized in unrestricted form (UB3LYP).[18,19] Previous work has shown that this hybrid functional can provide very reliable predictions of the state energies, structures, and vibrational frequencies of transition metal containing compounds.[20,21] The 6-311++G** basis set was used for N, O, and H, and the all-electron basis set of Wachters−Hay as modified by Gaussian was used for Sc.[22,23] The geometries were fully optimized, the harmonic vibrational frequencies were calculated with analytic second derivatives, and zero-point vibrational energies (ZPVE) were derived. Transition-state optimizations were done with the synchronous transit-guided quasi-Newton (STQN) method.[24]

## Results and Discussions

**Infrared Spectra.** The infrared spectra in the N−N and Sc−H stretching frequency regions from co-deposition of Sc atoms and $N_2/H_2O$ mixture in excess argon are shown in Figure 1, and the product absorptions are listed in Table 1. In addition to the ScNN (1902.0 cm$^{-1}$)[25] and HScOH (1482.6 cm$^{-1}$)[26,27] absorptions, new absorptions at 1953.2, 1944.2, 1884.3, 1832.9, 1831.0, 1487.9, 1476.9, 1442.8, and 1437.6 cm$^{-1}$ were observed.

* Corresponding author. E-mail: mfzhou@fudan.edu.cn.

10.1021/jp045414j CCC: $30.25 
Published on Web 12/31/2004

**TABLE 1: Infrared Absorptions ($cm^{-1}$) from Co-deposition of Laser-Ablated Scandium Atoms with $N_2/H_2O$ Mixtures in Excess Argon at 12 K**

| $^{14}N_2$ | $^{15}N_2$ | $D_2O$ | $H_2{}^{18}O$ | $^{14}N_2 + {}^{15}N_2$ | $^{14}N_2 + {}^{14}N^{15}N + {}^{15}N_2$ | assignment[a] |
|---|---|---|---|---|---|---|
| 1953.2 | 1889.5 | 1950.5 | 1953.0 | 1953.2, 1913.1, 1889.5 | 1953.2, 1936.9, 1934.2, 1923.8, 1921.7, 1919.3, 1913.1, 1904.4, 1889.5 | ($\eta^1$-NN)$_2$Sc(H)OH N−N str |
| 1944.2 | 1881.0 | 1941.0 | 1944.0 | 1944.2, 1905.8, 1881.0 | | ($\eta^1$-NN)$_2$Sc(H)OH site |
| 1884.3 | 1822.8 | 1879.1 | 1884.1 | 1884.3, 1822.8 | 1884.3, 1854.9, 1853.1, 1822.8 | ($\eta^1$-NN)Sc(H)OH N−N str |
| 1832.9 | 1772.5 | 1831.9 | 1832.8 | 1832.9, 1772.5 | 1833.0, 1803.1, 1772.5 | ($\eta^2$-N$_2$)Sc(H)OH N−N str |
| 1831.0 | 1770.5 | 1829.9 | 1830.9 | 1831.1, 1770.5 | 1831.1, 1801.0, 1770.5 | ($\eta^2$-N$_2$)Sc(H)OH site |
| 1487.9 | 1487.6 | 1071.8 | 1487.9 | | | ($\eta^2$-N$_2$)Sc(H)OH site |
| 1476.9 | 1476.6 | 1066.4 | 1476.9 | | | ($\eta^2$-N$_2$)Sc(H)OH Sc−H str |
| 1442.8 | 1442.0 | 1043.5 | 1442.8 | | | ($\eta^1$-NN)Sc(H)OH Sc−H str |
| 1437.6 | 1437.4 | 1038.0 | 1437.6 | | | ($\eta^1$-NN)$_2$Sc(H)OH Sc−H str |

[a] str = stretch.

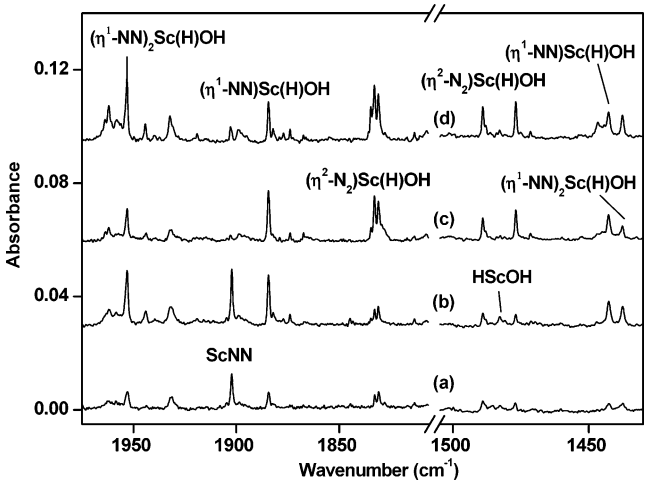


**Figure 1.** Infrared spectra in the 1805−1975 and 1430−1500 $cm^{-1}$ regions from co-deposition of laser-ablated Sc atoms with 0.2% $N_2$ and 0.05% $H_2O$ in argon at 12 K: (a) with 1 h of sample deposition, (b) after 25 K annealing, (c) after 20 min of $\lambda > 300$ nm irradiation, and (d) after 35 K annealing.

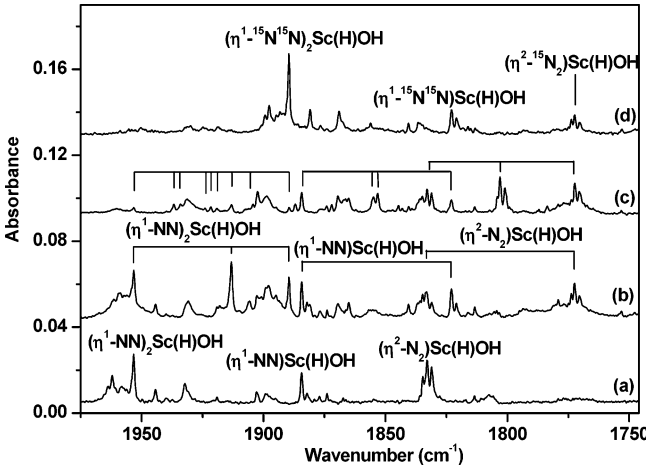


**Figure 2.** Infrared spectra in the 1745−1975 $cm^{-1}$ regions from co-deposition of laser-ablated Sc atoms with isotopic substituted $N_2$ and $H_2O$ samples in excess argon. Spectra were taken after 2 h of sample deposition followed by 30 K annealing: (a) 0.2% $^{14}N_2$ + 0.05% $H_2O$, (b) 0.15% $^{14}N_2$ + 0.15% $^{15}N_2$ + 0.05% $H_2O$, (c) 0.075% $^{14}N_2$ + 0.15% $^{14}N^{15}N$ + 0.075% $^{15}N_2$ + 0.05% $H_2O$, and (d) 0.2% $^{15}N_2$ + 0.05% $H_2O$.

These absorptions were only produced in the experiments when both the $N_2$ and $H_2O$ samples were employed. On the basis of their growth/decay characteristics measured as a function of changes of experimental conditions, these product absorptions can be grouped into three different product molecules. The 1884.3 and 1442.8 $cm^{-1}$ absorptions increased together on the initial 25 K annealing (trace b) and slightly decreased on subsequent $\lambda > 300$ nm irradiation (trace c) and 35 K annealing (trace d). The 1953.2 and 1437.6 $cm^{-1}$ absorptions also increased together on the 25 K annealing and decreased on $\lambda > 300$ nm irradiation, but recovered on 35 K annealing. The 1832.9/1831.0 and 1487.9/1476.9 $cm^{-1}$ doublets are very weak on sample deposition. These absorptions remained almost unchanged on the initial 25 K annealing but increased markedly on $\lambda > 300$ nm irradiation.

The experiments were repeated using the isotopically labeled $^{15}N_2/H_2O$, $N_2/D_2O$, $N_2/H_2{}^{18}O$, $N_2/H_2O + HDO + D_2O$, $^{14}N_2 + {}^{15}N_2/H_2O$, and $^{14}N_2 + {}^{14}N^{15}N + {}^{15}N_2/H_2O$ samples. The isotopic counterparts are also listed in Table 1. Figure 2 shows the spectra in the 1745−1975 $cm^{-1}$ region using different isotopic samples. The spectra in the 1430−1500 and 1025−1078 $cm^{-1}$ regions with the $N_2/H_2O + HDO + D_2O$ sample are illustrated in Figure 3.

**Calculation Results.** Quantum chemical calculations were performed on the potential product molecules. The optimized structures are shown in Figure 4. The total energies, vibrational frequencies, and intensities of various species involved in the $Sc/N_2/H_2O$ system are listed in Table 2.

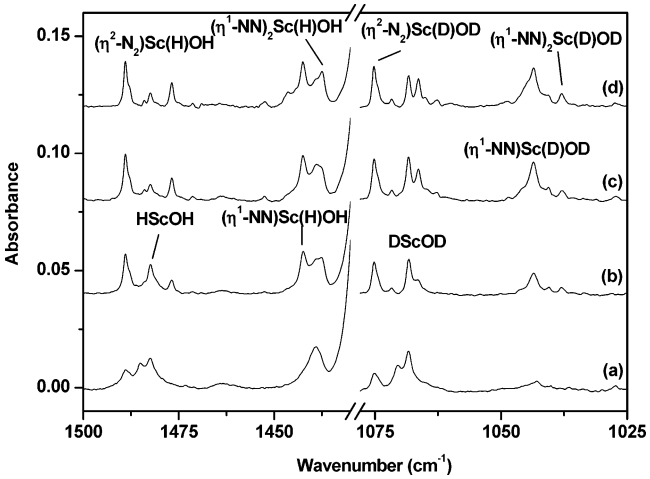


**Figure 3.** Infrared spectra in the 1430−1500 and 1025−1078 $cm^{-1}$ regions from co-deposition of laser-ablated Sc atoms with 0.2% $N_2$ and 0.05% $H_2O$ + 0.1% HDO + 0.05% $D_2O$ in argon at 12 K: (a) with 1 h of sample deposition, (b) after 25 K annealing, (c) after 20 min of $\lambda > 300$ nm irradiation, and (d) after 35 K annealing.

**($\eta^1$-NN)Sc(H)OH.** The bands at 1884.3 and 1442.8 $cm^{-1}$ are assigned to the ($\eta^1$-NN)Sc(H)OH molecule. The 1884.3 $cm^{-1}$ band exhibited very small isotopic shifts when the $N_2/D_2O$ and $N_2/H_2{}^{18}O$ samples were used but shifted to 1822.8 $cm^{-1}$ in the experiment with $^{15}N_2/H_2O$. The $^{14}N/^{15}N$ isotopic frequency ratio of 1.0337 is indicative of a N−N stretching vibration. In the

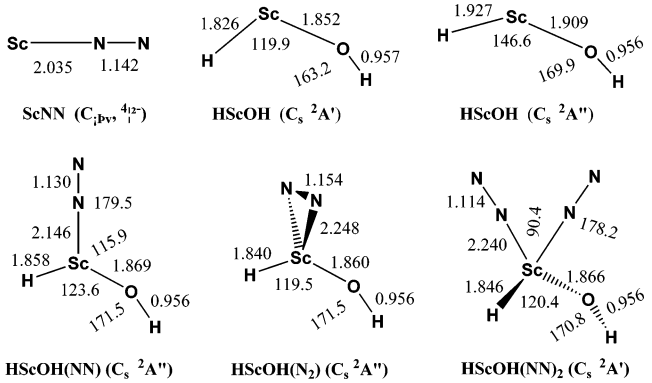


**Figure 4.** Optimized structures (bond lengths in angstroms and bond angles in degrees) of the experimentally observed reaction products.

experiment with a $^{14}N_2 + {}^{15}N_2/H_2O$ sample, only the 1884.3 and 1822.8 cm$^{-1}$ bands were observed, which indicates that only one $N_2$ is involved in the molecule. A quartet at 1884.3, 1854.9, 1853.1, and 1822.8 cm$^{-1}$ with approximately 1:1:1:1 relative intensities was produced when a $^{14}N_2 + {}^{14}N^{15}N + {}^{15}N_2/H_2O$ sample was used. This quartet feature implies that the two nitrogen atoms are inequivalent. The 1442.8 cm$^{-1}$ band shows no shift with $N_2/H_2{}^{18}O$ and very small shift (0.8 cm$^{-1}$) with $^{15}N_2/H_2O$. When the $N_2/D_2O$ sample was used, the 1442.8 cm$^{-1}$ band shifted to 1043.5 cm$^{-1}$, which gave a H/D isotopic frequency ratio of 1.3827. The band position and isotopic frequency ratio support the assignment of the 1442.8 cm$^{-1}$ band to a Sc−H stretching vibration.

Density functional calculations were performed to support the assignment. As shown in Figure 4, the ($\eta^1$-NN)S**c(**H)OH molecule was predicted to have a $^2$A″ ground state with a $C_s$ symmetry. The N−N and Sc−H stretching modes were computed at 2048.8 and 1507.3 cm$^{-1}$, which should be multiplied by 0.920 and 0.957 to fit the observed frequencies. The calculated $^{14}N/^{15}N$ isotopic frequency ratio of 1.0348 for the N−N stretching mode and the H/D ratio of 1.3959 for the Sc−H stretching mode agree well with the experimental ratios, 1.0337 and 1.3827. The calculation results also indicate that the N−N and Sc−H stretching modes have the largest IR intensities.

The ($\eta^1$-NN)S**c(**H)OH complex has been calculated by Hwang and Mebel at the B3LYP/6-31G** level of theory.[9] They predicted the ($\eta^1$-NN)S**c(**H)OH complex would have a $^2$A′ ground state which correlates to the ground-state HScOH ($^2$A′) + $N_2$. We note that their optimized geometry and relative stability with respect to ($\eta^2$-$N_2$)Sc**(**H)OH are almost the same as those of the present $^2$A″ ($\eta^1$-NN)Sc**(**H)OH complex. We suspect that the $^2$A′ state reported by Hwang and Mebel is actually the present reported $^2$A″ state, which correlates to the $^2$A″ first excited state of HScOH and $N_2$, as will be discussed below. The $^2$A′ state ($\eta^1$-NN)Sc**(**H)OH complex, which correlates to the ground-state HScOH and $N_2$, was predicted to be 7.5 kcal/mol less stable than the $^2$A″ state at the B3LYP/6-311++G** level.

**($\eta^2$-$N_2$)Sc(H)OH.** The present experiments provide evidence for another product with the ($N_2$)Sc(H)OH stoichiometry. The absorptions at 1832.9/1831.0 and 1487.9/1476.9 cm$^{-1}$ are assigned to the N−N and Sc−H stretching modes of the ($\eta^2$-$N_2$)Sc**(**H)OH complex at two trapping sites. The 1832.9/1831.0 cm$^{-1}$ doublet shifted to 1772.5/1770.5 cm$^{-1}$ with $^{15}N_2/H_2O$. The $^{14}N/^{15}N$ isotopic frequency ratio of 1.0341 also indicates a N−N stretching vibration. The band position suggests a side-bonded structure. No intermediate absorption was produced when the $^{14}N_2 + {}^{15}N_2/H_2O$ sample was used, whereas a triplet with intermediate at 1803.1/1801.0 cm$^{-1}$ was observed in the $^{14}N_2 + {}^{14}N^{15}N + {}^{15}N_2/H_2O$ spectra. These findings confirm that the molecule involves a $N_2$ subunit with two equivalent N atoms. The 1487.9/1476.9 cm$^{-1}$ doublet shows very small or no shift with either $^{15}N_2/H_2O$ or $N_2/H_2{}^{18}O$ samples but shifted to 1071.8/1066.4 cm$^{-1}$ with $N_2/D_2O$. The H/D isotopic frequency ratio is about the same as that of the Sc−H stretching mode of ($\eta^1$-NN)Sc(H)OH. No intermediate absorption was observed in the experiment with the $N_2/H_2O + HDO + D_2O$ sample, indicating the involvement of only one ScH subunit.

As shown in Figure 4, the ($\eta^2$-$N_2$)Sc**(**H)OH molecule was predicted to have a $^2$A″ ground state with a $C_s$ symmetry. The $N_2$ unit is side-bonded to the Sc center with the $ScN_2$ plane perpendicular to the HScOH plane. This structure was predicted to be 2.2 kcal/mol more stable than the $^2$A″ ($\eta^1$-NN)Sc(H)OH isomer, in accord with the previous theoretical predictions.[9] The N−N and Sc−H stretching modes were computed at 1964.3 and 1544.8 cm$^{-1}$. The N−N stretching mode is 84.5 cm$^{-1}$ lower, whereas the Sc−H stretching mode is 37.5 cm$^{-1}$ higher than those of the ($\eta^1$-NN)Sc(H)OH molecule, consistent with the experimental observations.

Both the ($\eta^1$-NN)S**c(**H)OH and ($\eta^2$-$N_2$)Sc(H)OH molecules have a $^2$A″ ground state and can be viewed as being formed by

**TABLE 2: Calculated Total Energies (hartrees, after Zero Point Energy Correction), Vibrational Frequencies (cm$^{-1}$), and Intensities (km/mol) of Various Species in the Sc/$N_2$/$H_2O$ System**

| | energy | frequency (intensity) |
|---|---|---|
| Sc ($^2$D) | −760.620 4572 | |
| $N_2$ ($^1\Sigma_g$) | −109.554 125 | 2444.9 |
| $H_2O$ ($^1A_1$) | −76.437 245 | 1602.3 (66); 3818.0 (9); 3923.2 (57) |
| $ScOH_2$ ($^2$A″) | −837.078 918 | 179.2 (157); 374.2 (26); 1560.4 (140); 3584.1 (543); 3685.0 (2); 324.1(6) |
| ScNN ($^4\Sigma$) | −870.179 458 | 254.3 (1); 394.5 (31); 1943.7 (1019) |
| HScOH ($^2$A′) | −837.155 718 | 325.4 (81); 351.0 (160); 372.2 (166); 717.1 (210); 1529.7 (512); 3953.7 (229) |
| HScOH ($^2$A″) | −837.142 830 | 170.1 (247); 409.1 (221); 425.0 (241); 659.6 (214); 1397.3 (413); 3962.3 (111) |
| $H_2OScNN$ ($^2$A″) | −946.643 197 | 21.4 (16); 53.2 (3); 204.4 (1); 214.9 (3); 283.3 (204); 313.1 (109); 371.2 (35); 379.0 (12); 1556.6 (125); 2032.0 (1872); 3579.8 (442); 3668.6 (4) |
| ($\eta^1$-NN)Sc(H)OH ($^2$A″) | −946.731 867 | 90.7 (3); 143.2 (182); 229.9 (6); 268.0 (62); 298.7 (177); 347.9 (19); 395.7 (282); 404.2 (65); 719.4 (325); 1507.3 (174); 2048.8 (991); 3966.0 (230) |
| ($\eta^2$-$N_2$)Sc(H)OH ($^2$A″) | −946.735 367 | 118.3 (4); 136.3 (51); 244.1 (153); 272.2 (183); 358.6 (12); 366.6 (0); 398.0 (305); 442.5 (72); 732.4 (302); 1544.8 (603); 3966.0 (235) |
| ($\eta^1$-NN)$_2$Sc(H)OH ($^2$A′) | −1056.304 461 | 48.8 (0); 82.6 (3); 83.2 (0); 188.7 (21); 221.0 (5); 241.4 (13); 251.9 (23); 279.2 (44); 282.7 (20); 293.8 (154); 321.3 (14); 364.0 (157); 395.4 (94); 715.3 (294); 1520.3 (674); 2090.1 (3048); 2241.4 (30); 3966.3 (227) |
| TS1 | −946.634 101 | |
| TS2 | −837.063 925 | |
| TS3 | −946.720 078 | |

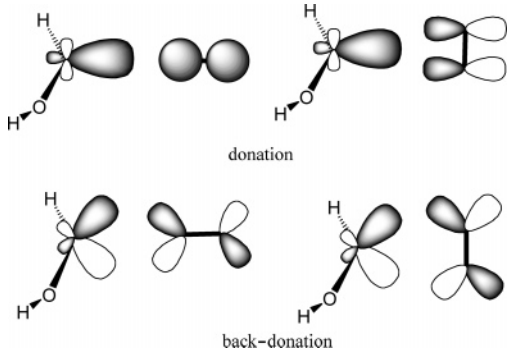


**Figure 5.** Principle orbital interactions in ($\eta^1$-NN)Sc(H)OH and ($\eta^2$-$N_2$)Sc(H)OH.

the interaction of a $^2A''$ HScOH fragment and a $N_2$ fragment. The interactions between HScOH and $N_2$ are dominated by the synergic donations of filled orbitals of $N_2$ into an empty acceptor orbital of HScOH and the back-donation of the HScOH electrons to the empty orbitals of $N_2$. The HScOH molecule has a $^2A'$ ground state with an electron configuration of (core) $(3a'')^2(12a')^2(13a')^1(4a'')^0$. The $^2A''$ state with electron configuration of (core) $(3a'')^2(12a')^2(4a'')^1(13a')^0$ was predicted to lie 8.1 kcal/mol higher in energy than the $^2A'$ ground state. As shown in Figure 5, the 13a′ orbital of HScOH is primarily a hybrid of the Sc 4s and $3d_{z^2}$ orbitals that is directed away from the H and O atoms. This orbital is the primary acceptor orbital for donation from the $N_2$ fragment. In ($\eta^1$-NN)Sc(H)OH, the filled $3\sigma_g$ molecular orbital of $N_2$ is the principal donor orbital. The filled $1\pi_u$ molecular orbitals of $N_2$ are also donor orbitals in ($\eta^2$-$N_2$)-Sc(H)OH. The 4a″ orbital of HScOH is primarily the Sc $3d_{xz}$ orbital that is mainly nonbonding. This a″ orbital is also polarized away from the H and O atoms. It can interact with the $\pi_g$ antibonding orbitals of $N_2$ in either end-on (($\eta^1$-NN)Sc-(H)OH) or side-on (($\eta^2$-$N_2$)Sc(H)OH) geometry. The back-donation of electron density into the antibonding $\pi$ orbitals of $N_2$ decreases the bond strength of the $N_2$ fragment. Consistent with this notion, the calculated N−N bond lengths in ($\eta^1$-NN)-Sc(H)OH and ($\eta^2$-$N_2$)Sc(H)OH are 1.130 and 1.154 Å, respectively, which are 0.034 and 0.058 Å longer than that of free $N_2$ calculated at the same level. Since both N atoms are coordinated to the Sc center, the interaction between $N_2$ and HScOH in ($\eta^2$-$N_2$)Sc(H)OH is stronger than that in ($\eta^1$-NN)Sc(H)OH. Therefore, the ($\eta^2$-$N_2$)Sc(H)OH structure is slightly more stable than the ($\eta^1$-NN)Sc(H)OH isomer. The weakening of the N−N bond also leads to a large red-shift of the N−N stretching frequencies of ($\eta^1$-NN)Sc(H)OH and ($\eta^2$-$N_2$)Sc(H)OH (calculated 2048.8 and 1964.3 $cm^{-1}$) relative to that of $N_2$ (calculated 2444.9 $cm^{-1}$). The orbitals of the HScOH fragment involved in the bonding (4a″ and 13a′) are primarily Sc-based orbitals and are mainly nonbonding; the bonding interactions only change the HScOH geometry slightly (Figure 4).

**($\eta^1$-NN)$_2$Sc(H)OH.** The absorptions at 1953.2 and 1437.6 $cm^{-1}$ maintained the same relative intensities throughout all the experiments and are assigned to the different vibrational modes of ($\eta^1$-NN)$_2$Sc(H)OH. The upper band shifted to 1889.5 $cm^{-1}$ with $^{15}N_2/H_2O$. The $^{14}N/^{15}N$ isotopic frequency ratio (1.0337) is characteristic of a N−N stretching vibration. The band position is blue-shifted from the N−N stretching modes of ScNN and the above-characterized ($\eta^1$-NN)Sc(H)OH molecules, which suggests a terminal N−N stretching vibration. In the experiment with $^{14}N_2 + {}^{15}N_2/H_2O$, a triplet at 1953.2, 1913.1, and 1889.5 $cm^{-1}$ was produced, indicating that two equivalent dinitrogens are involved in this mode. In the experiment with $^{14}N_2 + {}^{14}N^{15}N + {}^{15}N_2/H_2O$, seven intermediate absorptions at 1936.9, 1934.2, 1923.8, 1921.7, 1919.3, 1913.1, and 1904.4 $cm^{-1}$ were identified. These spectral features imply that the two nitrogen atoms in each $N_2$ subunit are inequivalent, and the molecule involves a Sc(NN)$_2$ subunit. The 1437.6 $cm^{-1}$ band shifted to 1038.0 $cm^{-1}$ in the $N_2/D_2O$ experiment. Both the band position and the H/D isotopic frequency ratio (1.3850) indicate that the 1437.6 $cm^{-1}$ band is due to a Sc−H stretching mode.

The identification of ($\eta^1$-NN)$_2$Sc(H)OH is supported by density functional theory (DFT) calculations. The molecule was predicted to have a $^2A'$ ground state with a $C_s$ symmetry, in which the two $N_2$ fragments lie in the same plane that is perpendicular to the HScOH plane. The two $N_2$ subunits are equivalent, and the N atoms in each $N_2$ are inequivalent. The antisymmetric N−N stretching and Sc−H stretching modes were computed at 2090.1 and 1520.3 $cm^{-1}$ with the calculated isotopic frequency ratios in good agreement with the experimental values. Geometry optimization was also performed with the two $N_2$ subunits in a side-bonded fashion. The calculation found that the side-bonded structure is slightly higher in energy than the terminal-bonded structure with the calculated spectral features that do not match the observed frequencies.

In contrast to ($\eta^1$-NN)Sc(H)OH and ($\eta^2$-$N_2$) Sc(H)OH, the ground state of ($\eta^1$-NN)$_2$Sc(H)OH correlates to the $^2A'$ ground-state HScOH and $2N_2$. As shown in Figure 6, the interactions in this complex involve electron donation from the bonding $\sigma$ orbital of $N_2$ to the empty 4a″ molecular orbital of HScOH and back-donation from the singly occupied 13a′ molecular orbital of HScOH to the antibonding $\pi^*$ molecular orbital of $N_2$. It seems that the donation dominates the interactions in ($\eta^1$-NN)$_2$-Sc(H)OH. The calculated N−N bond length in ($\eta^1$-NN)$_2$Sc(H)-OH (1.114 Å) is shorter, while the N−N stretching frequency is higher than those of ($\eta^1$-NN)Sc(H)OH and ($\eta^2$-$N_2$)Sc(H)OH.

The binding energies of $^2A''$ ($\eta^1$-NN)Sc(H)OH and ($\eta^2$-$N_2$)-Sc(H)OH were predicted to be 21.9 and 24.1 kcal/mol, respectively with respect to HScOH ($^2A''$) + $N_2$. Since the $^2A''$-state HScOH lies 8.1 kcal/mol above the $^2A'$ ground state, the binding energies with respect to HScOH ($^2A'$) + $N_2$ become 13.8 and 16.0 kcal/mol. The binding energy per $N_2$ in ($\eta^1$-NN)$_2$-Sc(H)OH was estimated to be 12.7 kcal/mol with respective to HScOH ($^2A'$) + $2N_2$.

**Reaction Mechanism.** Earlier studies on the reaction of Sc atoms with $H_2O$ showed that the ground-state Sc atoms inserted spontaneously into one of the O−H bonds of water to form the HScOH molecule in solid argon.[26,27] Previous study on the reaction of Sc atoms with $N_2$ produced ScNN.[25] Both the HScOH and ScNN absorptions were observed to increase on annealing in the present $Sc/N_2/H_2O$ experiments. The HScOH and ScNN could further react with $N_2$ or $H_2O$ to form the ($\eta^1$-NN)Sc(H)OH and ($\eta^2$-$N_2$)Sc(H)OH complexes, reactions 1 and 2.

$$\mathrm{HScOH}\ (^2A') + \mathrm{N_2}\ (^1\Sigma_g^+) \rightarrow (\eta^1\text{-NN})\mathrm{Sc(H)OH}\ (^2A'') \qquad \Delta E = -13.8\ \mathrm{kcal/mol} \quad (1a)$$

$$\mathrm{HScOH}\ (^2A') + \mathrm{N_2}\ (^1\Sigma_g^+) \rightarrow (\eta^2\text{-N}_2)\mathrm{Sc(H)OH}\ (^2A'') \qquad \Delta E = -16.0\ \mathrm{kcal/mol} \quad (1b)$$

$$\mathrm{ScNN}\ (^4\Sigma^-) + \mathrm{H_2O}\ (^1A_1) \rightarrow (\eta^1\text{-NN})\mathrm{Sc(H)OH}\ (^2A'') \qquad \Delta E = -72.3\ \mathrm{kcal/mol} \quad (2a)$$

$$\mathrm{ScNN}\ (^4\Sigma^-) + \mathrm{H_2O}\ (^1A_1) \rightarrow (\eta^2\text{-N}_2)\mathrm{Sc(H)OH}\ (^2A'') \qquad \Delta E = -74.5\ \mathrm{kcal/mol} \quad (2b)$$

As has been mentioned above, the ($\eta^1$-NN)Sc(H)OH and ($\eta^2$-$N_2$)Sc(H)OH complexes correlate with the electronically excited

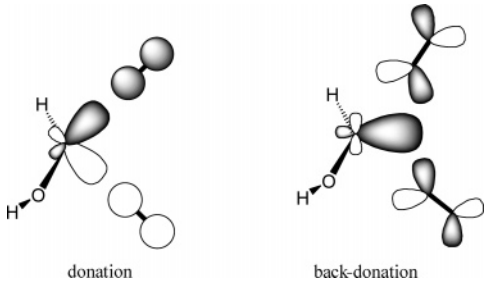


**Figure 6.** Principle orbital interactions in $(\eta^1\text{-NN})_2$Sc(H)OH.

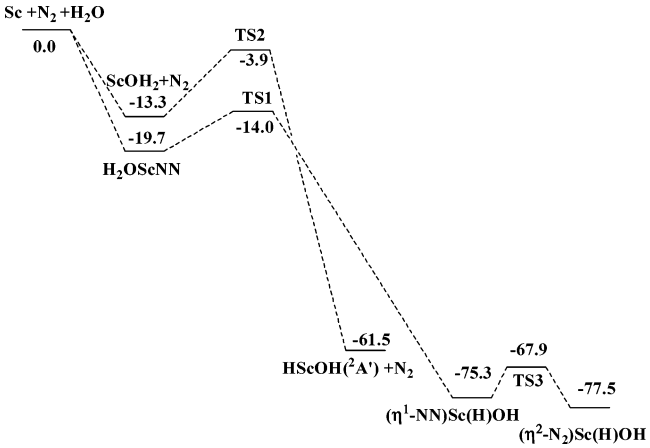


**Figure 7.** Potential energy profiles for the Sc + $N_2$ + $H_2O$ reactions (values in kilocalories per mole).

HScOH ($^2$A″) + $N_2$ reactants. Formation of $^2$A″ ($\eta^1$-NN)Sc(H)OH and ($\eta^2$-$N_2$)Sc(H)OH from the ground-state HScOH involves crossing or avoided crossing of the $^2$A′ and $^2$A″ potential energy surfaces and probably requires activation energy. Experimentally, the ($\eta^1$-NN)Sc(H)OH absorptions increased on annealing, whereas the ($\eta^2$-$N_2$)Sc(H)OH absorptions increased only on broad-band irradiation. This suggests that ($\eta^1$-NN)Sc(H)OH is mainly formed via reaction 2a, which was predicted to be quite exothermic. As shown in Figure 7, the reaction proceeds via the initial formation of a $H_2$OScNN complex, which was predicted to have a doublet ground state. Formation of ($\eta^1$-NN)Sc(H)OH from the $H_2$OScNN complex proceeds via a transition state (TS1). .TS1 lies 5.7 kcal/mol above the $H_2$OScNN complex., but is 14.0 kcal/mol lower in energy than the Sc + $N_2$ + $H_2O$ reactants. Since the formation of $H_2$OScNN is initially exothermic by about 19.7 kcal/mol, which is sufficient to surmount the energy barrier for the O−H bond insertion, the formation of ($\eta^1$-NN)Sc(H)OH from $H_2$-OScNN is spontaneous in solid argon. This also suggests that the $H_2$OScNN complex is a short-lived species, rapidly arranging to form the ($\eta^1$-NN)Sc(H)OH complex. Our calculations also indicated that the addition of $N_2$ increases the reactivity of Sc atom with respect to $H_2O$. The Sc atom insertion into $H_2O$ to form HScOH involves two processes (Figure 7): the initial formation of a $ScOH_2$ complex, which proceeds without any energy barrier, following the Sc atom insertion into one of the O−H bonds of $H_2O$ to form HScOH via a transition state (TS2).[28] This transition state lies 9.4 kcal/mol above the $ScOH_2$ complex and is only 3.9 kcal/mol lower in energy than the ground-state Sc + $H_2O$ reactants. Therefore, the energy barrier for the Sc atom insertion decreases about 4.7 kcal/mol by the addition of $N_2$.

As has been pointed out previously,[9] there is an energy barrier on the pathway connecting the ($\eta^1$-NN)Sc(H)OH and ($\eta^2$-$N_2$)-Sc(H)OH complexes. The transition state (TS3) was calculated to be 7.4 kcal/mol higher in energy than the $^2$A″ ($\eta^1$-NN)Sc-(H)OH complex, in good agreement with the value (7.3 kcal/mol) reported by Hwang and Mebel.[9] The ($\eta^2$-$N_2$)Sc(H)OH absorptions increased only upon broad-band irradiation, also suggesting that the formation of ($\eta^2$-$N_2$)Sc(H)OH requires some activation energy.

The $(\eta^1\text{-NN})_2$Sc(H)OH absorptions increased on annealing, indicating that the formation of $(\eta^1\text{-NN})_2$Sc(H)OH requires no activation energy. This complex could be formed either via the reaction of the ground-state HScOH with two $N_2$ molecules or via the reaction of ($\eta^1$-NN)Sc(H)OH with $N_2$. Both reactions were predicted to be exothermic.

$$\text{HScOH}\ (^2\text{A}') + 2\text{N}_2\ (^1\Sigma_g^-) \rightarrow (\eta^1\text{-NN})_2\text{Sc(H)OH}\ (^2\text{A}') \qquad \Delta E = -25.4\ \text{kcal/mol} \quad (3)$$

$$(\eta^1\text{-NN})\text{Sc(H)OH}\ (^2\text{A}'') + \text{N}_2\ (^1\Sigma_g^-) \rightarrow (\eta^1\text{-NN})_2\text{Sc(H)OH}\ (^2\text{A}') \qquad \Delta E = -11.6\ \text{kcal/mol} \quad (4)$$

## Conclusions

Hydridoscandium hydroxide dinitrogen complexes, ($\eta^2$-$N_2$)-Sc(H)OH and $(\eta^1\text{-NN})_x$Sc(H)OH ($x$ = 1, 2), have been studied by matrix isolation infrared absorption spectroscopy and density functional theory calculations. These dinitrogen complexes were produced via the reactions of laser-ablated scandium atoms and $N_2/H_2O$ mixtures in solid argon matrix. Both the ($\eta^1$-NN)Sc-(H)OH and ($\eta^2$-$N_2$)Sc(H)OH complexes were predicted to have a $^2$A″ ground state with $C_s$ symmetry and can be viewed as being formed by the interaction of the first excited state $^2$A″ HScOH and $N_2$ fragments. The $\eta^2$-coordinated complex is slightly more stable than the $\eta^1$-coordinated structure. The $(\eta^1\text{-NN})_2$Sc(H)OH complex has a $^2$A′ ground state which correlates to the $^2$A′ ground-state HScOH and $2N_2$.

**Acknowledgment.** We greatly acknowledge financial support from NSFC (Grant 20125311) and the NKBRSF (Grant 2004CB719501) of China.

## References and Notes

(1) Buchel, H.; Moretto, H. H.; Woditsh, P. *Inductrielle Anorganische Chemie*; Wiley/VCH: Weinheim, Germany, 1999; Vol. 3.
(2) Hidai, M.; Mizobe, Y. *Chem. Rev.* **1995**, *95*, 1115.
(3) Richards, R. L. *Coord. Chem. Rev.* **1996**, *154*, 83.
(4) Hidai, M. *Coord. Chem. Rev.* **1999**, *185*−*186*, 99.
(5) Siegbahn, P. E. M.; Blomberg, M. R. A. *Chem. Rev.* **2000**, *100*, 421.
(6) Sekusak, S.; Frenking, G. *J. Mol. Struct. (THEOCHEM)* **2001**, *541*, 17.
(7) Hwang, D. Y.; Mebel, A. M. *J. Phys. Chem. A* **2003**, *107*, 2865.
(8) Hwang, D. Y.; Mebel, A. M. *J. Phys. Chem. A* **2003**, *107*, 5092.
(9) Hwang, D. Y.; Mebel, A. M. *Chem. Phys. Lett.* **2003**, *375*, 17.
(10) Kushto, G. P.; Souter, P. F.; Chertihin, G. V.; Andrews, L. *J. Chem. Phys.* **1999**, *110*, 9020.
(11) Andrews, L.; Bare, W. D.; Chertihin, G. V. *J. Phys. Chem. A* **1997**, *101*, 8417.
(12) Andrews, L.; Bare, W. D.; Chertihin, G. V. *J. Phys. Chem. A* **1998**, *102*, 2561.
(13) Elustondo, F.; Mascetti, J. *J. Phys. Chem. A* **2000**, *104*, 3572.
(14) Chen, M. H.; Zhou, M. F.; Zhang, L. N.; Qin, Q. Z. *J. Phys. Chem. A* **2000**, *104*, 8627.
(15) Zhou, M. F.; Zhang, L. N.; Qin, Q. Z. *J. Phys. Chem. A* **2001**, *105*, 6407.
(16) Chen, M. H.; Wang, X. F.; Zhang, L. N.; Yu, M.; Qin, Q. Z. *Chem. Phys.* **1999**, *242*, 81.
(17) Frisch, M. J.; Trucks, G. W.; Schlegel, H. B.; Scuseria, G. E.; Robb, M. A.; Cheeseman, J. R.; Montgomery, J. A., Jr.; Vreven, T.; Kudin, K. N.; Burant, J. C.; Millam, J. M.; Iyengar, S. S.; Tomasi, J.; Barone, V.; Mennucci, B.; Cossi, M.; Scalmani, G.; Rega, N.; Petersson, G. A.; Nakatsuji, H.; Hada, M.; Ehara, M.; Toyota, K.; Fukuda, R.; Hasegawa, J.; Ishida, M.; Nakajima, T.; Honda, Y.; Kitao, O.; Nakai, H.; Klene, M.; Li,

X.; Knox, J. E.; Hratchian, H. P.; Cross, J. B.; Adamo, C.; Jaramillo, J.; Gomperts, R.; Stratmann, R. E.; Yazyev, O.; Austin, A. J.; Cammi, R.; Pomelli, C.; Ochterski, J. W.; Ayala, P. Y.; Morokuma, K.; Voth, G. A.; Salvador, P.; Dannenberg, J. J.; Zakrzewski, V. G.; Dapprich, S.; Daniels, A. D.; Strain, M. C.; Farkas, O.; Malick, D. K.; Rabuck, A. D.; Raghavachari, K.; Foresman, J. B.; Ortiz, J. V.; Cui, Q.; Baboul, A. G.; Clifford, S.; Cioslowski, J.; Stefanov, B. B.; Liu, G.; Liashenko, A.; Piskorz, P.; Komaromi, I.; Martin, R. L.; Fox, D. J.; Keith, T.; Al-Laham, M. A.; Peng, C. Y.; Nanayakkara, A.; Challacombe, M.; Gill, P. M. W.; Johnson, B.; Chen, W.; Wong, M. W.; Gonzalez, C.; Pople, J. A. *Gaussian 03*, Revision B.05; Gaussian, Inc.: Pittsburgh, PA, 2003.

(18) Becke, A. D. *J. Chem. Phys.* **1993**, *98*, 5648.

(19) Lee, C.; Yang, E.; Parr, R. G. *Phys. Rev. B* **1988**, *37*, 785.

(20) Bauschlicher, C. W., Jr.; Ricca, A.; Partridge, H.; Langhoff, S. R. In *Recent Advances in Density Functional Theory*; Chong, D. P., Ed.; World Scientific Publishing: Singapore, 1997; Part II.

(21) Siegbahn, P. E. M. Electronic Structure Calculations for Molecules Containing Transition Metals. Advances in Chemical Physics XCIII, 1996; Wittborn, A. M. C., Costas, M., Blomberg, M. R. A., Siegbahn, P. E. M. *J. Chem. Phys*. **1997**, *107*, 4318.

(22) McLean, A. D.; Chandler, G. S. *J. Chem. Phys.* **1980**, *72*, 5639.

(23) Krishnan, R.; Binkley, J. S.; Seeger, R.; Pople, J. A. *J. Chem. Phys*. **1980**, *72*, 650.

(24) Head-Gordon, M.; Pople, J. A.; Frisch, M. *Chem. Phys. Lett*. **1988**, *153*, 503.

(25) Chertihin, G. V.; Andrews, L.; Bauschlicher, C. W., Jr. *J. Am. Chem. Soc*. **1998**, *120*, 3205.

(26) Kauffman, J. W.; Hauge, R. H.; Margrave, J. L. *J. Phys. Chem*. **1985**, *89*, 3541.

(27) Zhang, L. N.; Dong, J.; Zhou, M. F. *J. Phys. Chem. A* **2000**, *104*, 8882.

(28) Hwang, D. Y.; Mebel, A. M. *Chem. Phys. Lett*. **2001**, *341*, 393.